

Slow-Positron Emission from Metal Surfaces

A. P. Mills, Jr., P. M. Platzman, and B. L. Brown
Bell Laboratories, Murray Hill, New Jersey 07974
 (Received 4 August 1978)

Slow (< 5 eV) positrons (e^+) are observed emanating from clean (submonolayer contaminated) single-crystal metal surfaces which are being bombarded by 0.1–3-keV e^+ . A portion of the emitted slow e^+ from Al(100) has a narrow range of energies and a temperature-dependent intensity which suggests that these e^+ are thermalized in the bulk and have a negative work function $\phi_+ = -0.2 \pm 0.1$ eV. A higher-energy portion of the slow- e^+ spectrum has a temperature-independent intensity attributable to nonthermalized e^+ .

The generation of slow positrons from radioactive sources¹⁻⁴ and the utilization of these positrons to study fundamental properties of positronium in vacuum^{5,6} and a variety of phenomena in gases⁷⁻⁹ and at solid surfaces^{10,11} is by now an active field of research. The interaction of moderate-energy positrons with solids at some point involves the strong coupling of these particles with surfaces on the angstrom scale. To date, most experiments to probe the behavior of positrons at solid surfaces have involved complex and possibly contaminated surfaces. Thus, the detailed nature of the microscopic mechanism involved, for example, in slow positron emission and absorption has remained unknown. In this Letter, we would like to report the first observation of slow e^+ emission from well-characterized surfaces.

A 100-mCi source of Co⁵⁸ and Pt moderator produces a flux of slow e^+ in vacuum (10^{-9} Torr) at one end of a 3-m-long, 30-cm-i.d., ~ 150 -G solenoid. The source and moderator can be biased positive to yield a beam of e^+ with a well-defined energy up to 3 keV. The e^+ beam is initially moving parallel to the magnetic induction \vec{B} along the axis of the solenoid. After acceleration, the beam is $\vec{E} \times \vec{B}$ deflected through two off-axis apertures and then back to the axis. The beam passes through a final on-axis aperture and experiences a 25-eV deceleration as it enters the beam tube which leads to the ultrahigh-vacuum (10^{-10} Torr) target chamber. Since the $\vec{E} \times \vec{B}$ drift is independent of the direction of the e^+ velocity component v_{\parallel} parallel to B , the e^+ beam structure is totally absorbent to re-emitted e^+ returning from the target.

The annihilation of e^+ at the target is detected by a 3-in. \times 3-in. NaI(Tl) scintillator located behind the target. The target samples are mounted on a heater stage which can be moved to different positions for ion bombardment and analysis by low-energy electron diffraction (LEED) and Auger spectroscopy. The integral longitudinal

($\frac{1}{2}mv_{\parallel}^2$) energy spectrum of slow e^+ emitted by the target is measured by recording the annihilation rate versus target bias using a multiscaler. To ensure that re-emitted e^+ will travel back to the source region and be absorbed, the target is located behind a positively biased grid. When the target is biased positive, all emitted e^+ are swept away and the count rate is low. As the bias becomes more negative, more and more low-energy e^+ are attracted back to the target and the counting rate increases.

Figure 1(a) shows the integral energy spectra of the slow-positron yield from a single-crystal sample of Al(100) which has been cleaned with an argon ion beam and annealed at a temperature of 600°C for a period of 10 min. The sample shows well-defined LEED spots and the Auger spectrum shows the surface to be less than 0.2% contaminated with oxygen. Surface conditions were checked both before and after the e^+ yield experiments and no notable deterioration of the surface took place. The yield curves shown in Fig. 1(a)

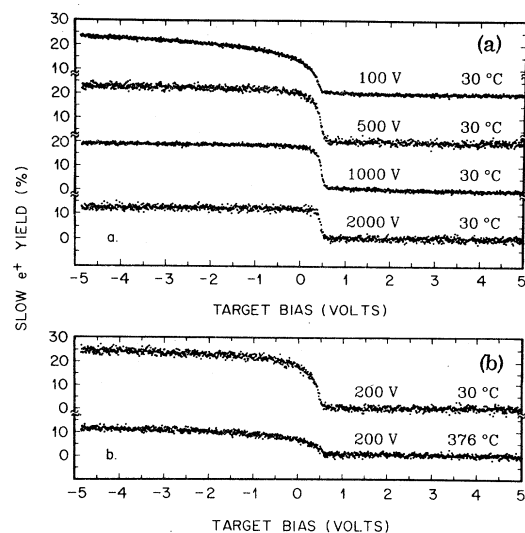


FIG. 1. Background-corrected retarding-potential spectra of slow e^+ emitted by Al(100). The target temperature and incident e^+ energy are indicated.

are for several different incident e^+ energies ranging from 100 to 2000 eV. On those runs, the sample was kept at a constant temperature of 30°C. The target bias is measured with respect to the positively biased (4.87 V) Cu grid. All of the curves show a steep rise near zero bias. More specifically, they are made up of a very rapid jump whose width (ΔE) is of the order 0.2 eV superimposed on a broader rise. The overall yield of slow positrons decreases as the incident energy E increases while the fraction of the rise in the slowly varying part of the curves also decreases.

The slow-positron yield is temperature dependent in a way shown in Figs. 1(b) and 2. Figure 1(b) shows, for $E=200$ eV, spectra taken at 30 and 376°C. The spectrum at the higher temperature has lost its sharp rise and is completely characterized by its broad increase. Figure 2 shows that the e^+ yield for Al with $E=1000$ eV decreases to zero as the temperature is increased to 400°C. The yield y is defined as the difference between the counting rate for negative bias (-0.63 to -4.82 V) and the rate for positive bias (+1.62 to +5.36 V) divided by the rate for negative bias.

Figure 3 shows that y decreases with increasing incident energy E in a way which is very sim-

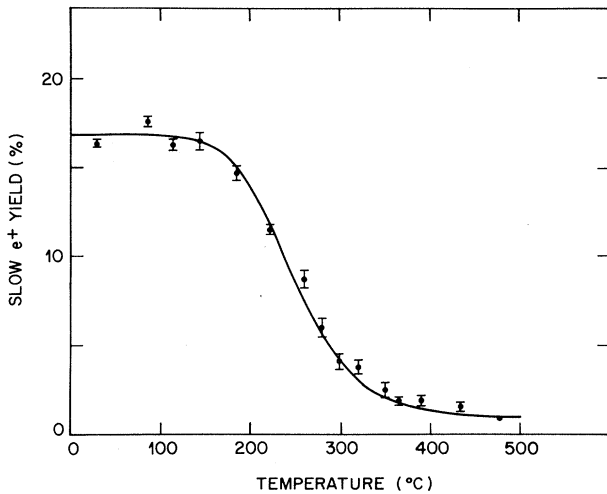


FIG. 2. Slow- e^+ yield y from Al(100) vs temperature; $E=1000$ eV. The curve is fitted Arrhenius function $y = (y_0 + zy_\infty)/(1+z)$ where $z = z_0 \exp(-T/T_0)$. The best-fit parameters are $y_0 = 16.9$, $y_\infty = 0.9$, $z_0 = 3.52 \times 10^6$, and $T_0 = 7840 \pm 160$ K with a rather poor $\chi^2/\nu = 31.6/11$ which can be attributed to temperature uncertainties. To correct for background, the data of this figure should be multiplied by 1.15.

ilar to the variation of the positronium yield¹¹ with E . If we ignore the two data points at the lowest energies, at which the positrons appear to be significantly nonthermal in the bulk (see discussion below), the 30°C data of Fig. 3(b) is fitted by the function

$$y(E) = y_0(E/E_0 + 1)^{-1} \quad (1)$$

with $y_0 = 0.39 \pm 0.01$, and $E_0 = 720 \pm 30$ V. Equation (1) was derived in Ref. 11 assuming (1) that the incident e^+ stop in the target with an exponential distribution whose mean depth is linear in E ; (2) that the e^+ then diffuse through the target in order to reach the surface.

All these results for Al can be understood on the basis of quite simple arguments if we keep in mind that the present measurements as a function of bias give us a direct measure of $\frac{1}{2} m v_{\parallel}^2$ for e^+ which are emitted from the surface. In addition we must assume, as seems reasonable, that the e^+ emerge with random direction. Thus the width in bias voltage is a direct measure of the spread in energy of the e^+ being emitted. Positrons with energies $E > 200$ eV enter the sample and begin losing energy to the electrons in the metal. Typical loss processes involve plasmon emission and some interband and core-level excitation. The mean free path for these processes varies from a low of perhaps 10 Å at 200 eV to a high of 200 Å for a few thousand eV e^+ . After $\sim 10^{-14}$ sec, the positrons have energies in the eV range and they probably come to equilibrium

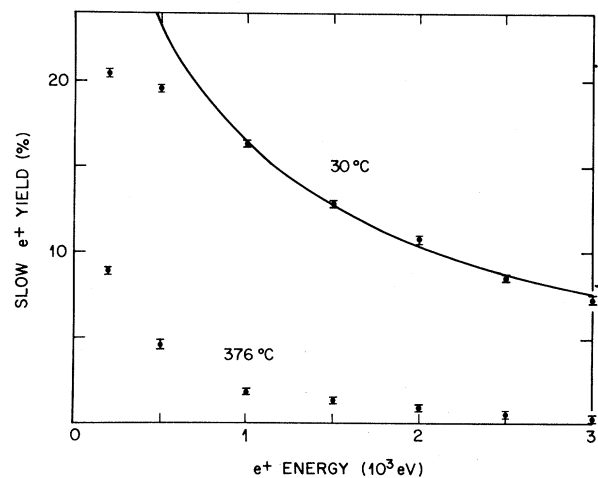


FIG. 3. Slow- e^+ yield y from Al(100) vs incident e^+ energy. The curve through the 30°C data is a fit of Eq. (1) to the five highest-energy data points. To correct for background, the data of this figure should be multiplied by 1.15.

with the lattice in about 10^{-12} sec.

While in the process of thermalizing with the lattice, the positrons diffuse toward the surface¹¹ with a diffusion constant of order $D \approx 0.1 \text{ cm}^2 \text{ sec}^{-1}$. A typical nonthermal e^+ will diffuse about 30 \AA in 10^{-12} sec, its thermalization time. Thus, positrons in the 1000-eV range, which have stopping distances in the hundred-angstrom range, will be thermalized when they reach the surface. At the surface, some of the e^+ will form positronium (Ps)^{10,11} and some will be emitted (if the work function is negative) with an energy spread of $\frac{1}{2}m v_{\parallel}^2$ which is a direct measure of the equilibrium work function. It is also possible that as much as 10% of the thermal e^+ reaching the surface become trapped in a surface state.¹² A large portion of low incident energy ($E \approx 200 \text{ eV}$) e^+ is not thermalized before reaching the surface. These e^+ are emitted with an energy spread characteristic of their nonthermal distribution. Thus we are able to understand the shape of the curves in Fig. 1 which show that the amount of nonthermal e^+ emitted increases as E decreases. The amplitude of the curves is a measure of the branching ratio for slow- e^+ emission versus Ps formation at the surface.

The above discussion makes it plausible that the 10%–90% width of the retarding-potential curves equals the e^+ work function ϕ_+ when the incident e^+ energy is $E > 1000 \text{ eV}$. In Fig. 4, we show some $E = 1000 \text{ eV}$ yield curves for clean single-crystal Al(100), Cr, and Si(100). These data give the e^+ work function for three materials: Al, $\phi_+ = -0.2 \pm 0.1 \text{ eV}$; Cr, $\phi_+ = -1.7 \pm 0.2 \text{ eV}$; Si, $\phi_+ = -1.0 \pm 0.2 \text{ eV}$. These are no experiments on clean surfaces to compare with; however, Pendayala *et al.*⁴ and Cherry² both observed slow e^+ from their Cr samples. Nieminen and Hodges¹³ calculate for Cr $\phi_+ = -2.2 \text{ eV}$; Hodges and Stott¹⁴ calculate for Al $\phi_+ = +0.7 \text{ eV}$.

The reason for the temperature effect in Fig. 3 is not yet certain. The data can be fitted by an Arrhenius plot with an activation energy of $0.68 \pm 0.02 \text{ eV}$, a value which is similar to the vacancy activation energy¹⁵ in bulk Al. It is also observed¹⁶ that the Ps formation probability has a behavior complementary to the slow- e^+ yield versus temperature. A possible model would be that at low temperatures, e^+ are not trapped in vacancies and slow- e^+ emission occurs. At high temperatures, all the e^+ become trapped and slow- e^+ emission becomes energetically impossible, although Ps emission is not forbidden. Of course, nonthermal positrons are not trapped

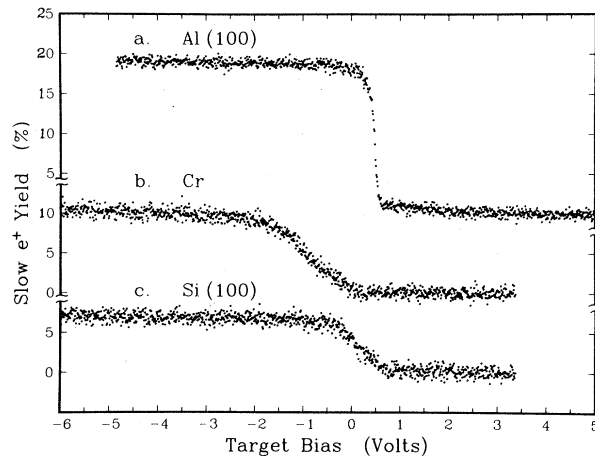


FIG. 4. Background-corrected retarding potential curves of the slow- e^+ spectra emitted by Al(100), Cr, and Si(100) for 1000-eV incident e^+ . The Al showed a (100) LEED pattern; the surface contamination in monolayers was estimated by Auger analysis to be 1% Sn, <0.2% O₂, and <1% C. The Cr was evaporated onto mica and proved to be contaminated with 25% C. No LEED pattern was observed although the orientation is supposed to be (110). The Si sample was cleaned by heating to near the melting point. The differences in the target bias voltages at which the curves begin to rise equal the contact-potential (electron work function) differences for the three targets.

and the persistence, in the presence of defects, of the nonthermal spread of emitted e^+ is explained.

We have thus demonstrated that the positron work function is negative in several clean single-crystal samples. A detailed understanding of this work function and the possible implications of slow-positron emission, positronium yield, low-energy positron reflection, and low-energy positron capture to form positronium awaits further theoretical and experimental developments.

As a first step in making use of these findings, an Al(100) crystal, bombarded with 1-keV Ar ions and annealed *in situ* at 590°C, has been used as a slow- e^+ moderator. With a beam energy of 19.4 eV, the 10%–90% energy width of the slow- e^+ beam is $0.16 \pm 0.02 \text{ eV}$ in agreement with the data of Fig. 4. The 63% width $0.09 \pm 0.02 \text{ eV}$, is as narrow as the beam produced by the coated boron moderator of Stein, Kauppilla, and Roellig.¹⁷ The total counting rate of $2 \times 10^3 \text{ sec}^{-1}$ implies that the slow- e^+ conversion efficiency is $\epsilon = (3 \pm 1) \times 10^{-5}$. While this efficiency is comparable to the best reported values,⁷ it is small when

compared with estimates^{1,18,19} which predict $\epsilon \approx 10^{-3}$. For example, if we approximate a β^+ spectrum by $N(E) = 12E_m^{-4}E(E - E_m)^2$ and integrate over the slow- e^+ yield $y(E)$ of Eq. (1), we find

$$\epsilon = \int_0^{E_m} y(E)N(E)dE \cong 4y_0E_0/E_m.$$

Using a β^+ end-point energy $E_m = 500$ keV and the values of y_0 and E_0 measured for Al, we have $\epsilon = 10^{-3}$ for a 2π geometry. The order of magnitude discrepancy between these theoretical and experimental values for ϵ may mean that the β^+ spectrum is deficient in low-energy e^+ because of self-absorption in the source. In any case, further improvements in the efficiency of slow- e^+ moderators seem possible.

The authors are pleased to thank Dr. T. M. Rice, Dr. D. R. Hamman, and Dr. J. E. Rowe for interesting discussions.

¹L. Madansky and F. Rasetti, Phys. Rev. **79**, 397 (1950).

²W. Cherry, Ph.D. dissertation, Princeton University, 1958 (unpublished), available from University Microfilms, Ann Arbor, Mich.

³D. G. Costello, D. E. Groce, D. F. Herring, and J. W. McGowan, Phys. Rev. B **5**, 1433 (1972), and references therein.

⁴S. Pendayala, D. Bartell, F. E. Girouard, and J. W. McGowan, Phys. Rev. Lett. **33**, 1031 (1974).

⁵K. F. Canter, A. P. Mills, Jr., and S. Berko, Phys.

Rev. Lett. **34**, 177 (1975); A. P. Mills, Jr., S. Berko, and K. F. Canter, Phys. Rev. Lett. **34**, 1541 (1975).

⁶D. W. Gidley, P. W. Zitzewitz, K. A. Marko, and A. Rich, Phys. Rev. Lett. **37**, 729 (1976).

⁷K. F. Canter, P. G. Coleman, T. C. Griffith, and G. R. Heyland, J. Phys. B **5**, L167 (1972), and **6**, L201 (1973), and Appl. Phys. **3**, 249 (1974).

⁸J. S. Tsai, L. Lebow, and D. A. L. Paul, Can. J. Phys. **54**, 1741 (1976), and references therein.

⁹T. S. Stein, W. E. Kauppilla, V. Pol, J. H. Smart, and G. Jesion, Phys. Rev. A **17**, 1600 (1978), and references therein.

¹⁰K. F. Canter, A. P. Mills, Jr., and S. Berko, Phys. Rev. Lett. **33**, 7 (1974).

¹¹A. P. Mills, Jr., to be published.

¹²A. Gainotti and C. Ghezzi, J. Phys. C **5**, 779 (1972); C. H. Hodges, J. Phys. C **8**, 1849 (1975); R. Nieminen and M. Manninen, Solid State Commun. **15**, 403 (1974); C. H. Hodges and M. J. Stott, Solid State Commun. **12**, 1153 (1973).

¹³R. M. Nieminen and C. H. Hodges, Solid State Commun. **18**, 1115 (1976).

¹⁴C. H. Hodges and M. J. Stott, Phys. Rev. B **7**, 73 (1973).

¹⁵I. K. MacKenzie, T. L. Khoo, A. B. McDonald, and B. T. A. McKee, Phys. Rev. Lett. **19**, 946 (1967); B. T. A. McKee, W. Triftshäuser, and A. T. Stewart, Phys. Rev. Lett. **28**, 358 (1972).

¹⁶Data to be published.

¹⁷T. S. Stein, W. E. Kauppilla, and L. O. Roellig, Phys. Lett. **51A**, 327 (1975).

¹⁸W. C. Keever, B. Jaduszliwer, and D. A. L. Paul, in *Atomic Physics*, edited by S. J. Smith and G. K. Walters (Plenum, New York, 1972), pp. 561-571.

¹⁹A. P. Mills, Jr., and L. N. Pfeiffer, Phys. Lett. **63A**, 118 (1977).

φ^4 Domain Walls in Thin Ferromagnetic Films: Occurrence of a Novel Critical Point

K. R. Subbaswamy^(a) and D. L. Mills

Department of Physics, University of California, Irvine, California 92717

(Received 7 August 1978)

We consider the magnetic-field (H) dependence of the magnetization (M) of a thin low-anisotropy ferromagnetic film near T_c placed on a magnetically hard substrate well below its Curie temperature. Our mean-field-theory analysis uses a free-energy functional analogous to the φ^4 Lagrangian for a complex scalar field used recently in a description of solitons in charge-density-wave condensates. We find a novel critical point in the appropriate M - H plane and comment on its accessibility to experimental investigation.

There is currently a great deal of interest in physical manifestations of solitary-wave solutions that emerge from certain classes of nonlinear equations.¹ The Bloch wall in a ferromagnet with uniaxial anisotropy offers, in its most elementary form,² a physical realization of the

soliton associated with the sine-Gordon equation. More recently Rice, Bishop, Krumhansl, and Trullinger³ have suggested that solitons could provide a means for conductivity in commensurability-pinned charge-density-wave (CDW) condensates.⁴